

## Kinetic Study of Phase Transformation of Al-Zn-Mg-Cu Alloy during Quenching Process

Yanjun Xie, Tietao Zhou, Peiying Liu, Chaoli Ma

Department of Materials Science and Engineering, Beijing University of Aeronautics and Astronautics,  
Beijing, China

Quench sensitivity exists in thick plate of Al-Zn-Mg-Cu alloy. The precipitation of second phase during quenching process had an impact on the final properties of this alloys. In this paper, taking 7050 aluminium alloy as an example, the quenching process was analyzed by kinetic rules of phase transformation using a model of heterogeneous nucleation and growth. Reasonable assumptions and parameters were confirmed based on thermodynamics. Yield strength was calculated by volume fraction and mean radius of precipitates. The feasibility of this model was validated by experiment. It was found that the volume fraction of precipitates dropped dramatically with the rising of cooling rate, but it had finite effect if the cooling rate reached faster than 20°C/s. The number of  $\eta$  precipitates decreased with increase of cooling rate, and  $\eta$  phase did not exist in the matrix if the cooling rate during quenching process reached 56°C/s. Taking into account yield strength and distortion affected by quenching, a critical cooling rate was analyzed and ascertained at last.

**Key words:** *quenching process; Al-Zn-Mg-Cu alloy; kinetic study; precipitation*

### 1. Introduction

Al-Zn-Mg-Cu alloy is widely used in aeronautic structure materials for high strength to weight ratios [1]. The mechanical properties of this material depend on the size and distribution of precipitates. Quench sensitivity exists in thick plate of this aluminium alloy. That is, the cooling rate varies along the short horizontal section during quenching process. Many coarse equilibrium  $\eta$  particles precipitate along grain boundaries and dislocations due to the slower cooling rate from the solution heat treatment temperature in the core. This reduces the solutes available for aging hardening. Meanwhile, the vacancy concentration is also decreased, which is unfavorable for homogenous nucleation. Thus, the mechanical properties in the core of thick plate decrease [2,3]. Experimental study [3] also found that the precipitation during different cooling rates had an impact on the properties of Al-Zn-Mg-Cu alloys. The behavior of precipitation during quenching process has not been studied enough nowadays. In order to indicate the relationship between different cooling rates during quenching process and the change of precipitation, in this paper, taking 7050 aluminium ally as an example, the quenching process was analyzed by kinetic rules of phase transformation using a model of heterogeneous nucleation and growth. The aim of this work is to determine a reasonable cooling rate, and to evaluate the effect of different cooling rate on the size and distribution of precipitates during quenching process.

### 2. Model Description

#### 2.1 Calculation of volume fraction of precipitates

The precipitation of second phase in Al-Zn-Mg-Cu alloy is controlled by diffusion. It is a heterogeneous nucleation and growth process along grain boundaries and dislocations during quenching process. If considered this process from kinetic rules of phase transformation, the precipitation of second phase can be divided into three parts: nucleation, growth and coarsening. Because of the very short time of quenching process, we can regard that the precipitation only experienced nucleation and growth. The two processes are carried out at the same time.

It is feasible to neglect the impact of incubation time during heterogeneous nucleation [4, 5]. The

nucleation rate can be expressed as Eq. 1 during quenching process [4].

$$\dot{N} = N_0 \exp\left(-\frac{\Delta G_{het}^*}{RT}\right) \exp\left(-\frac{Q}{RT}\right) \quad (1)$$

Where  $N_0$  is the atomic number in unit volume.  $\Delta G_{het}^*$  is the critical activate energy of heterogeneous nucleation.  $Q$  is the activate energy of diffusion.

A rational  $\Delta G_{het}^*$  can be expressed as Eq. 2 based on classical nucleation theory and ignore the elastic strain energy between nuclear and matrix [4, 6].

$$\Delta G_{het}^* = \frac{(A^*)^3}{(RT)^2 [\ln(X_m / X_i)]^2} \quad (2)$$

Where  $X_i$  is the mole fraction of solute in the matrix at a certain temperature.  $A^*$  is a constant related to nuclear location, and has the same dimension with the critical activate energy of nucleation ( $J / mol$ ).  $X_m$  is the mean solute mole fraction in the matrix. It can be expressed as Eq. 3 during quenching process.

$$X_m = \frac{X_0 - fX_p}{1 - f} \quad (3)$$

$X_p$  is the mole fraction of solute in precipitates.

By using the definition of activate energy, a combination of Eq. 1 and Eq. 2 gives:

$$\dot{N} = N_0 \exp\left[-\left(\frac{A^*}{RT}\right)^3 \left(\frac{1}{\ln(X_m / X_i)}\right)^2\right] \exp\left(-\frac{Q}{RT}\right) \quad (4)$$

We can define the nuclear rate during quenching process by Eq. 4. The shape of precipitates can be regarded as spherical during the whole dynamic calculation. Therefore, the growth rate can be expressed as [4]:

$$\frac{dr}{dt} = \frac{X_m - X_i}{X_p - X_i} \frac{D}{r} = \frac{\varepsilon^2}{2r} \quad (5)$$

$D$  is the diffusion coefficient of solute atoms. It can be defined as  $D = D_0 \exp(-Q / RT)$  by diffusion theory.  $r$  is the current radius of precipitates.  $\varepsilon$  is the thickening constant[4], defined as:

$$\varepsilon = \sqrt{2D \frac{(X_m - X_i)}{(X_p - X_i)}} \quad (6)$$

The final volume fraction of precipitates during quench process can be calculated by Eq. 7:

$$f = \frac{4\pi}{3} \sum_{j=1}^n \dot{N} \Delta t (r_{j,n})^3 \quad (7)$$

$r_{j,n}$  is the final radius after quenching process nucleated at  $j$  time. The growth process can be expressed as [4]:

$$r_{j,k+1} = r_{j,k} + \frac{\varepsilon^2}{2r_{j,k}} \Delta t \quad (8)$$

The initial nucleation radius is [4]:

$$r_{j,j} = \varepsilon \sqrt{\Delta t} \quad (9)$$

## 2.2 Calculation of yield strength

The yield strength can be divided into three parts, strength of the matrix- $\sigma_0$ , the contribution of solution hardening- $\sigma_s$  and the contribution of precipitation hardening- $\sigma_p$ . It can be expressed as[7]:

$$\sigma_{total} = \sigma_0 + \sigma_s + \sigma_p \quad (10)$$

In this paper, yield strength of the matrix  $\sigma_0$  can be expressed by yield strength of hard-state pure aluminium. The contribution of solution to the yield strength is calculated as [7]:

$$\sigma_s = KX_s^{2/3} \quad (11)$$

$K$  is a constant.  $X_s$  is mole fraction of solute in the matrix. The contribution of precipitates to the yield strength can be expressed as [8, 9]:

$$\sigma_p = f_i \sigma_b \quad (12)$$

$f_i$  is the volume fraction affected by grain boundaries and dislocations. An assumption was made that the dislocation by-pass the precipitates, so  $\sigma_b$  can be expressed as [9]:

$$\sigma_b = \sqrt{\frac{6}{\pi}} \beta M \mu b \frac{f^{1/2}}{\bar{R}} \cong 0.7 M \mu b \frac{f^{1/2}}{\bar{R}} \quad (13)$$

$M$  is Taylor factor.  $\mu$  is the shear modulus.  $b = 3.3$  [9].  $f$  is the volume fraction of precipitates.  $\bar{R}$  is the mean radius of precipitates.

### 3. Experiment

7050-T7451 commercial aluminium alloy was used in experiment. The composition of this alloy is shown in table 1. The alloy was machined to block sample  $20\text{mm} \times 20\text{mm} \times 5\text{mm}$ . In order to measure the cooling curve during quenching process, a hole ( $\phi 1\text{mm} \times 10\text{mm}$ ) was drilled at one side of the sample and K type thermocouple was inserted in it. The sample was dissolved for 1 hour at  $470^\circ\text{C}$  in salt-bath furnace, and quenched into cold water, boiled water and air respectively. The transfer time was less than 5 seconds. The cooling curves during quenching process were recorded by Temperature detecting device. Vickers hardness was measured by the load of 1kg. Each data represents an average of six measurements.

Table 1 The chemical composition of experimental alloy

Chemical	Si	Fe	Cu	Mn	Mg	Zn	Ti	Zr
W (%)	0.05	0.10	2.3	0.01	2.2	6.1	0.02	0.11

### 4. Kinetic Analysis of Phase Transformation in Experiment

#### 4.1 Determination of kinetic parameters

The equilibrium volume fraction of different precipitates of 7050 at different temperature is calculated by Thermo-calc thermodynamic software. The results are shown in Fig. 1.

As we can see from Fig. 1, the precipitates of 7050 aluminium alloy at room temperature are  $S$ ,  $T$ ,  $MgZn_2$ ,  $Al_3Zr$ .  $MgZn_2$  phase has the largest number. Due to the volume fraction of  $S$ ,  $T$ ,  $MgZn_2$  at the same order of magnitude, the three precipitates are considered in the calculation of phase transformation.  $X_i$ ,  $X_0$ ,  $X_p$  in Eq. 2 and Eq. 3 represent mole fraction of Mg in matrix, initial alloy and precipitates respectively.  $X_0 = 0.026$ .  $X_p$  can be defined as 0.318 after considering all of the three precipitates. In order to determine the change of  $X_i$  with temperature, the mole fractions of Mg in the matrix are calculated at different temperature. The function fitting is done about the relationship of  $X_i$  and temperature. The function is obtained as Eq. 14:

$$X_i = 1.2 \times 10^{-7} T^2 - 7.093 \times 10^{-5} T + 0.0113305 \quad (14)$$

As we can see from Fig. 2, the fitting curve has an agreement with the calculated data about the mole fraction of Mg in the matrix at different temperature.

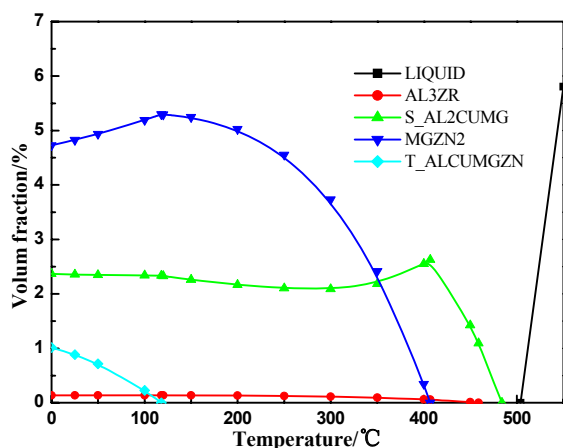


Fig. 1 Precipitates of 7050 at different temperature

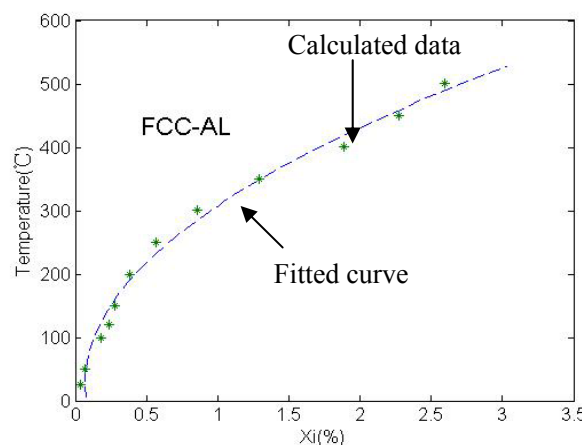


Fig. 2 The relationship between Xi and temperature

Three quenching mediums were used in the experiment, including cold water, boiled water and air. Cooling curves (Fig. 3) in different quenching mediums are recorded through the temperature detecting device. The detecting interval is 0.04s. This interval is also accepted during the calculation of phase transformation in Eq.7.

Other parameters used in kinetic calculation of phase transformation present in Table 2.

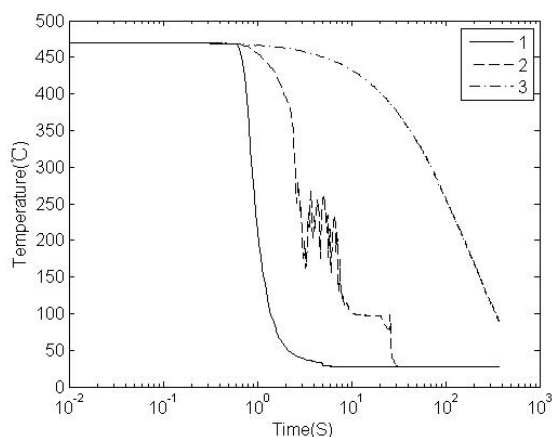


Fig. 3 Cooling curves at different quench mediums (1 cold water, 2 boiled water, 3 air)

Table 2 Parameters in the kinetic calculation of phase transformation

Parameter	Value	Comments
$A^*$ (J / mol)	$1.2758 \times 10^{-4}$	Obtained by[9]
$N_0$	$6.02 \times 10^{28}$	Calculated by Al
$Q$ (J / mol)	$1.205 \times 10^5$	Obtained by[10]
$D_0$	$1.49 \times 10^{-5}$	Obtained by[10]
$K$ (MPa)	840	Obtained by[9]
$f_i$	0.2	Calculated by [5,9]
$\sigma_0$ (MPa)	120	Obtained by[8]
$M$	2	Obtained by[9]
$\mu$ (GPa)	2.7	Obtained by[8]

## 4.2 Result and validation

The volume fraction of precipitates and the nuclear rate during quenching process are calculated by application of kinetic rules of phase transformation. The nuclear rate and volume fraction of precipitates during quenching process are shown in Fig. 4.

At the early stage of quenching process, due to the higher degree of super saturation in the matrix, the driving force of precipitation becomes greater. The diffusion velocity becomes faster as a result of relatively higher temperature. So the volume fraction of precipitates increases dramatically because of the higher nucleation and growth rate. At the late period of quenching process, the diffusion velocity, nuclear rate and growth rate become slow due to the relatively lower temperature. Therefore the volume fraction of precipitates change slowly and ultimately tends to a certain value.

The volume fraction, mean radius and whole number of precipitates quenched in different mediums present at table 3. The mean radius of precipitates has the same value with the Ref. [11] observed by transmission electron microscopy. However, as we can see from table 3, the mean radius of precipitates quenched in air is smaller than quenched in boiled water. A reasonable explanation is given by Fig. 5.

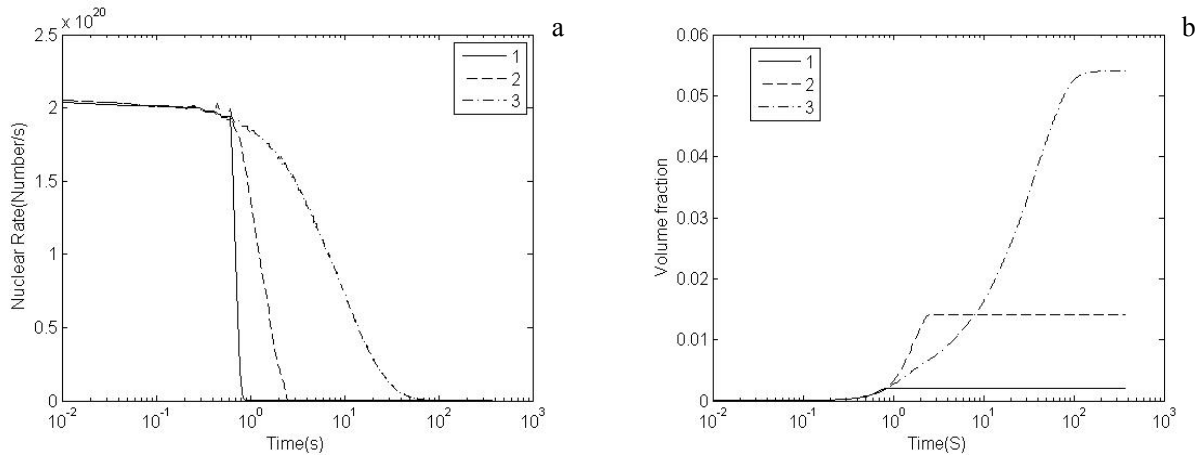


Fig. 4. (a) The nuclear rate during quenching process. (b) The volume fraction of precipitates during quenching process. (1 cold water, 2 boiled water, 3 air)

In order to validate the feasibility of the kinetic methods of phase transformation, yield strength was calculated by Eq. 10-13. The experimental yield strength was obtained by 3 times the Vickers hardness. Yield strength is 3 times Vickers hardness has been proved by A. Deschamps through experiments [9]. The calculated and experimental results present in table 4. The calculated results are approximate to the experimental data and the calculated error is less than 5%. So we can conclude that this method can be used in the calculation of precipitation during quenching process.

Table 3 the results after quenching in different mediums

Quench medium	$f$	$\bar{R}$ (nm)	Number of precipitates
Cold water	0.0020	14.195	1.4195e20
Boiled water	0.0142	22.259	2.6881e20
Air	0.0540	16.868	2.1063e21

Table 4 Comparison of calculated results and experiment data

Quench medium	Yield strength	Yield strength(calculated)
Cold water	264.6MPa	270.1MPa
Boiled water	290.1MPa	279.3MPa
Air	331.2MPa	314.6MPa

### 5. Optimization of Quenching Process

Based on the kinetic methods of phase transformation, the volume fraction and mean radius of precipitates were calculated at different cooling rates during quenching process (Fig. 5).

As we can see, in the low cooling rate condition (less than  $20^\circ\text{C/s}$ ), the volume fraction dropped dramatically with the development of cooling rate during quenching process, but it will have finite effect if the cooling rate reach faster than  $20^\circ\text{C/s}$ . In order to present a suitable cooling rate. According to the Refs. [11] and [12], we can regard that precipitates which has a radius more than 30nm( $\eta$  phase) has disadvantages to the final performance of Al-Zn-Mg-Cu alloy. According the formula of growth rate of precipitates during aging process [5]:

$$v = \frac{X_0 - X_i}{X_p - X_i} \sqrt{\frac{D}{t}} \tag{15}$$

We can calculate that the radius of precipitates can grow up 0.834nm after T6 aging ( $120^\circ\text{C}$ , 24h). The volume fraction of  $\eta$  phase after aging can be calculated at different quenching rates (table 5). We can see that the calculated result is near with experimental data [11]. The results show that  $\eta$  phase does not exist in the matrix after aging if the quenching cooling rate becomes greater than  $56^\circ\text{C/s}$ . The yield strength will not be improved if the cooling rate is further increased, however, serious stress and distortion will be increasing. So if the cooling rate during quenching process is greater than  $56^\circ\text{C/s}$ , it will have a disadvantage to the overall properties of Al-Zn-Mg-Cu alloy.

From Fig. 5 we can see that the mean radius of precipitates is decreasing with the rising of cooling rate if the mean cooling rate is greater than  $1.1^\circ\text{C/s}$ . However, if the mean cooling rate is

less than  $1.1\text{ }^{\circ}\text{C/s}$ , the mean radius of precipitates will be increasing with the rising of cooling rate. That is because the number of precipitates increases dramatically in very slow cooling rate. For example, as we can see from table. 3, the number of precipitates after air cooling is almost ten times of the number of precipitates after cooling at cold water or boiled water. This makes the mean radius of precipitates decreased.

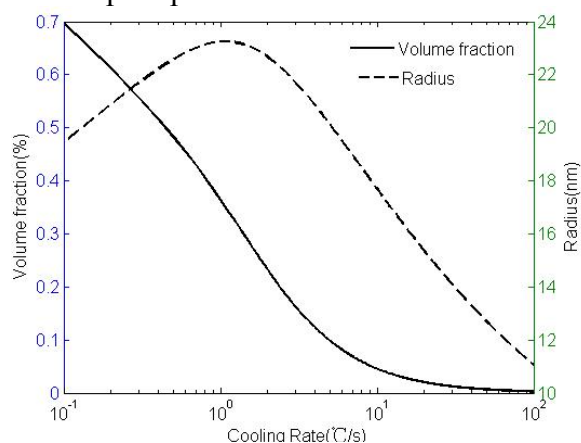


Fig. 5 The change of volume fraction and mean radius of precipitates with different quenching cooling rate

Table 5 Volume fraction of  $\eta$  phase in the precipitates after aging at different quenching cooling rate

Quenching cooling rate ( $^{\circ}\text{C/s}$ )	volume fraction of $\eta$ (%) (calculated)	volume fraction of $\eta$ (%)[11]
60	0	0
56	0	—
55	0.28	—
50	1.1	—
40	2.85	2.1
30	5.14	—
20	6.98	5.6

## 6. Summary and Conclusions

- 1) The volume fraction, mean radius and number of precipitates after different cooling rate during quenching process were calculated. The results were validated by experimental data.
- 2) Reasonable assumption of the kinetic model and the mole fraction of Mg in the matrix and precipitates were ascertained based on thermodynamics.
- 3) The volume fraction and mean radius of precipitates at different cooling rates were calculated. The results show that volume fraction of precipitates dropped dramatically with the development of cooling rate during quenching process, but it has finite effect if the cooling rate reached faster than  $20\text{ }^{\circ}\text{C/s}$ . The critical cooling rate that  $\eta$  phase does not exist in the matrix after aging is  $56\text{ }^{\circ}\text{C/s}$ .

## Reference

- [1] J. S. Robinson, R. L. Cudd, D. A. Tanner and G. D. Dolan: Journal of Materials Processing Technology. 119(2001) 261-267.
- [2] Gang Sha and Alfred Cerezo: Acta Materialia. 52(2004) 4503- 4516.
- [3] Jose Luis Cavazos and Rafael Colas: Material Science and Engineering. A363(2003) 171-178.
- [4]  $\Phi$ . Grong and H. R. Shercliff: Progress in Materials Science. 47(2002)195-196.
- [5] D. A. Porter and K. E. Easterling: Phase Transformations in metals and alloys. (Alden Press, Oxford,1981)pp. 280-287.
- [6] A. Deschamps, F. Livet and Y. Bréchet: Acta Mater. 47(1998)281.
- [7] Kocks. U. F, Argon. A. S and Ashby. M. F: Prog Mater Sci. 19(1975)1.
- [8] F. S. Pan and D. F. Zhang. Application of aluminium alloy. (Chemical Industry Press, Beijing, 2006) p. 298.
- [9] A. Deschamps, F. Livet and Y. Bréchet: Acta mater. 47(1998)293-305.
- [10] Y. Du, Y. A. Chang, B. Y. Huang, W. P. Gong, Z. P. Jin, H. H. Xu, Z. H. Yuan, Y. Liu, Y. H. He and F. Y. Xie: Materials Science and Engineering. 363(2003)140-151.
- [11] Y. Zhang. The study of quench sensitivity of 7050 aluminium alloy. (Master's thesis, Central South University. 2008)p: 51.
- [12] Q. C. Meng, X. G. Fan, S. Y. Ren, X. M. Zhang and B. Y. Zhang: Transactions of Nonferrous Metals Society of China. 16(2006)s1356-s1361.